Available online at www.sciencedirect.com

SCIENCE DIRECT®

Journal of Nuclear Materials 346 (2005) 16–23

journal of nuclear materials

www.elsevier.com/locate/jnucmat

The inhibiting effects of hydrogen on the corrosion of uranium dioxide under nuclear waste disposal conditions

M.E. Broczkowski [1], J.J. Noël, D.W. Shoesmith *

Department of Chemistry, The University of Western Ontario, 1151 Richmond Street, London, Ont., Canada N6A 5B7

Abstract

A number of electrochemical experiments were employed to investigate the effects of hydrogen on the corrosion of UO_2 under nuclear waste disposal conditions. A combination of corrosion potential (E_{CORR}) measurements and cyclic voltammetry have indicated that dissolved hydrogen can polarize the UO_2 surface to reducing potentials; i.e., to E_{CORR} values more negative then those observed under anoxic (argon-purged) conditions. A comparison of the behaviours of SIMFUEL specimens with and without incorporated noble metal ε-particles indicates that these particles may act as catalytic electrodes for H_2 oxidation, $H_2 \leftrightarrow 2e^- + 2H^+$. It is the galvanic coupling of these particles to the UO_2 matrix which suppresses the fuel corrosion potential.

PACS: 82.55; 82.45

1. Introduction

Many countries rely on electricity generated from nuclear power. With the use of nuclear power comes the responsibility of radioactive waste disposal. One option under consideration by Canada is burying the spent fuel 500–1000 m deep in the granitic rock of the Canadian Shield [1]. The CANDU fuel bundles would be placed in dual-walled containers with an outer layer of copper and an inner layer of carbon steel. Copper is chosen since it is thermodynamically stable under exposure to an anoxic environment such as that anticipated in the repository, while steel will be used for its strength and rigidity. These containers would be placed in the disposal vault and the vault backfilled with compacted bentonite clay and crushed rock. Failure of a container would lead to the contact of groundwater with both the fuel wasteform and the carbon steel inner shell. Since environmental oxidants will be rapidly consumed by waste container corrosion and mineral/biochemical oxidation processes [2], they will not exert any significant influence on fuel corrosion. By contrast, radiolytic oxidants will be produced directly in the environment immediately adjacent to the wetted fuel surface. The prospects for long-term containment using copper containers are very good, and corrosion models predict only minimal damage, insufficient to cause failure, will be incurred [4,5]. However, it is judicious to analyze the consequences for the fuel in the unlikely event of failure. A reasonable assumption is that the fuel will not be wetted while γ/β radiation fields are significant, Fig. 1, (i.e., the

---

* Corresponding author. Tel.: +1 519 661 2111; fax: +1 519 661 3022.

E-mail address: dwshoesm@uwo.ca (D.W. Shoesmith).

[1] Co-corresponding author.

doi:10.1016/j.jnucmat.2005.04.070

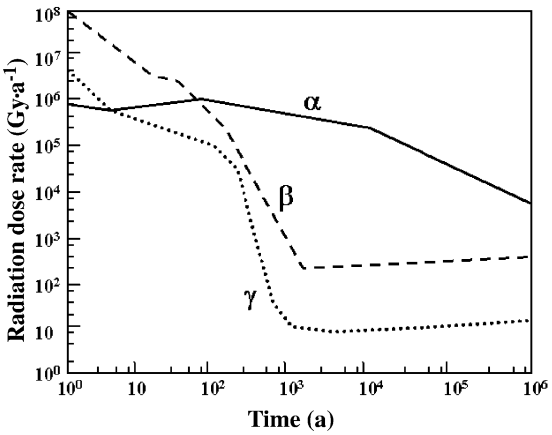

Fig. 1. Alpha (α), beta (β), and gamma (γ) radiation dose rates as a function of time calculated for water in contact with a CANDU fuel bundle with a burn-up of 721 GJ × kg^{-1}U [3].

container will last a minimum of 1000 years) and that, consequently, only the effects of α-radiolysis need be considered.

Recently, a model based on electrochemical principles that predicts the influence of α-radiolysis on fuel behaviour inside a failed waste container, was published [6]. The essential reactions in this model are illustrated in Fig. 2. At the fuel surface, oxidizing conditions leading to corrosion will be maintained by the α-radiolysis of water to produce H_2O_2 and O_2. At the steel surface, the anoxic corrosion of carbon steel can produce Fe^{2+} and H_2 by the reactions,

$$Fe + 2H_2O \rightarrow Fe^{2+} + 2OH^- + H_2 \tag{1}$$

$$3Fe + 4H_2O \rightarrow Fe_3O_4 + 4H_2 \tag{2}$$

In sealed repositories, the corrosion of carbon steel should cause substantial hydrogen pressures, leading to dissolved hydrogen concentrations in the 10^{-2}–10^{-1} mol × L^{-1} range. This introduces the possibility that H_2, produced by the corrosion of the steel, will scavenge the H_2O_2 produced by the α-radiolysis of water at the fuel surface by reaction to produce H_2O. This would limit fuel corrosion, thereby delaying radionuclide release.

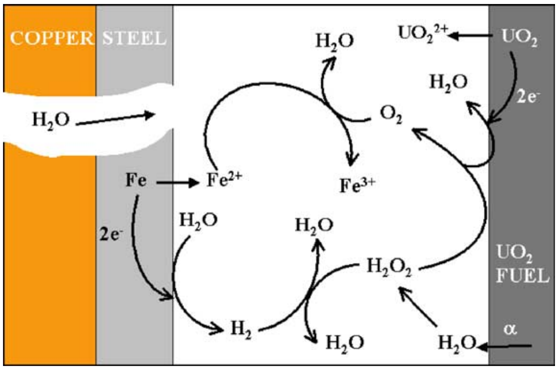

Fig. 2. Schematic showing the corrosion scenario inside a failed nuclear waste container.

The expected behaviour of a UO_2 surface as a function of surface redox condition (expressed as a corrosion potential, E_{CORR}) is summarized in Fig. 3. The corrosion potential is that potential at which the current for the anodic oxidation and/or dissolution of UO_2 is balanced by the current for the cathodic reduction of reacting oxidants (e.g., H_2O_2 and O_2). The chemical composition of the fuel surface and the ranges of different chemical/electrochemical behaviours have been determined using voltammetry, photodeflection spectroscopy, photocurrent spectroscopy, and X-ray photoelectron spectroscopy (XPS) [7,8]. The onset of observable oxidation occurs around −450 mV (vs SCE), the lowest potential for which an increase in U^V content of the fuel surface can be observed by XPS [8]. Over the potential range −450 to ≈0 mV, the ratio of U^V/U^{IV} in the fuel surface increases due to the formation of a thin surface oxide layer (2–8 nm). For potentials greater than 0 mV, the formation of a U^{VI} species occurs on the fuel surface [8].

Electrochemical studies coupled to photodeflection spectroscopy measurements detected dissolution at potentials as low as ≈−300 mV [9]. This value reflects a detection limit, and it is judicious to assume that dissolution can commence as soon as oxidation of the fuel surface ($U^{IV} \rightarrow U^V$), as defined by the XPS analysis, becomes possible. Based on these studies, we can claim

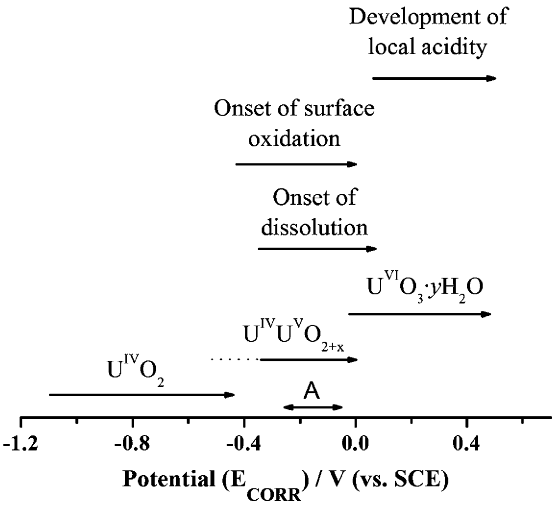

Fig. 3. Composition and corrosion behaviour of UO_2 as a function of the UO_2 corrosion potential.

that the corrosion of UO_2 does not occur for E_{CORR} values below −450 mV.

The bar marked A in Fig. 3 indicates the range of fuel E_{CORR} values predicted by a mixed potential model [6] from first contact with water (neglecting any influence of β/γ radiolysis effects). A comparison of this prediction to the threshold for oxidation/dissolution (corrosion) indicates that the surface redox condition of the fuel is predicted to always be in the range where corrosion is feasible. However, this model prediction does not include any consideration of the possible influence of hydrogen.

Spent fuel leaching studies in the presence of H_2 have shown it to have a very strong influence on radionuclide leaching and fuel corrosion rates [10], and recent studies have demonstrated a decrease in corrosion rate of over four orders of magnitude (compared to the rate under oxidizing conditions) for experiments in the presence of 1 atm (0.8 mmol × L^{-1} dissolved) H_2 [11]. These authors suggested this influence could be due to one, or both, of the following processes: (i) the reductive effect of hydrogen radicals, produced by a catalytic effect of the UO_2 surface on H_2 decomposition, on the fuel corrosion process; (ii) the scavenging of radiolytic oxidants by reaction with H_2. This second process is consistent with the predictions of standard radiolysis models [12] which calculate that moderate hydrogen concentrations ($\leqslant 10^{-5}\,\mathrm{mol} \times \mathrm{L}^{-1}$) are sufficient to suppress H_2O_2 production.

Electrochemical and surface analytical evidence exists to demonstrate the suppression of fuel oxidation by H_2 in the presence of α [13] and γ [14] radiation. Using XPS, Sunder et al. [13] showed that, at a temperature of 100 °C, the presence of dissolved H_2 suppressed the oxidation process,

$$UO_2 \rightarrow UO_{2+x} \rightarrow UO_3 \cdot yH_2O \tag{3}$$

driven by α radiolysis. Using external gamma sources and a H_2 pressure of 5 MPa, King et al. [14] found the corrosion potential of a UO_2 electrode suppressed to ≈−700 mV (vs SCE), a value well below that for the onset of UO_2 oxidation (≈−450 mV, Fig. 3). These last results suggest that H_2 not only consumes oxidants produced by gamma radiolysis, but also directly reduces the UO_2 surface. Since molecular H_2 is expected to be chemically slow to react at temperatures below 100 °C, it was argued that this reducing effect required the radiolytic production of hydrogen radicals ($H^{\bullet}$), which subsequently reduce the fuel surface.

The key requirement (if H_2 is to be made reactive) appears to be its decomposition to produce the reactive $H^{\bullet}$ species. However, if waste container failure is delayed for many thousands of years, it is unlikely that this will be achievable by the influence of radiation. We have, therefore, been studying the possibility that the fuel surface will be catalytic for the production of $H^{\bullet}$, and, hence, rendered immune to corrosion in the presence of a sufficient concentration of H_2. If such an effect can be demonstrated then it can legitimately be claimed that the release of those radionuclides contained within the fuel matrix will be extremely slow under failed container conditions.

2. Experimental

2.1. Electrode materials and preparation

Experiments were performed on SIMFUEL electrodes because this material is fabricated to reproduce the key properties of spent fuel without the radiation fields. The electrodes were cut from 1.5 at.% SIMFUEL pellets fabricated by Atomic Energy of Canada Limited (Chalk River, Ontario, Canada). SIMFUEL is an unirradiated analogue of used nuclear fuel, produced by doping the UO_2 matrix with a series of stable elements (Ba, Ce, La, Mo, Sr, Y, Rh, Pd, Ru, Nd, and Zr) in proportions appropriate to simulate the chemical effects caused by in-reactor irradiation [15,16]. The microstructure of SIMFUEL truly reflects that of a typical CANDU fuel pellet with polygonal, equiaxed UO_2 grains, 8–15 μm in size, and a density that is 97% of the theoretical value. As a consequence of this doping procedure, holes are injected into the 5f band, due to the substitution of trivalent rare-earth species for U^{IV} in the UO_2 fluorite lattice. This leads to an increase in oxide conductivity. The noble metal elements (Mo, Ru, Rh, and Pd), insoluble in the oxide lattice, congregate in metallic ε-particles. This phase consists of small, spherical precipitates (0.5–1.5 μm diameter) uniformly distributed in the UO_2 matrix [15]. The SIMFUEL used in these studies mimics UO_2 fuel irradiated to 1.5 at.% burn-up. Two samples were used, one with, and one without ε-particles.

Slices ≈3 mm thick and 12 mm in diameter were cut from the SIMFUEL. A thin layer of Cu was electroplated on one side of each slice to facilitate electrical contact to an external measuring device. A small round steel disc (≈5 mm thick, 10 mm diameter) was glued to the backside of each SIMFUEL slice with conducting silver epoxy, and attached to a threaded titanium shaft. Each electrode was then set in a sealing resin so that only one circular face of the electrode would be exposed to solution. Any exposed titanium and steel were painted with Amercot 90 HS resin to prevent any metal–solution contact.

2.2. Electrochemical cell and equipment

Experiments were conducted using a three-electrode, three-compartment electrochemical cell. The reference electrode was a commercial saturated calomel electrode (SCE), while the counter electrode was a platinum foil with a surface area of 13 cm^2, spot-welded to a platinum wire. The cell was housed in a grounded Faraday cage to minimize external sources of noise. Experiments at higher H_2 pressures were conducted in an electrochemical cell constructed within a Hasteloy pressure vessel with a PTFE liner [17]. The pressure vessel volume was 1 L, of which about 400 mL was filled with 0.1 mol × L^{-1} KCl solution prepared with ultrapure Millipore water (18.2 MΩ × cm). The remainder of the vessel was purged of oxygen with ultra high purity (UHP) argon gas. The reference electrode used within the pressure vessel was a custom-made silver/silver chloride electrode (Ag/AgCl). The potential of this electrode relative to the saturated calomel electrode is 40 mV at 25 °C. A Solartron model 1287 potentiostat was used to control applied potentials and to record current responses. Corrware™ software (supplied by Scribner Associates) was used to control the instruments and to analyze the data.

2.3. Electrode preparation and solutions

Prior to the start of each experiment, the electrode was polished with 220 grit, and then 1200 grit SiC paper and rinsed with de-aerated water. All solutions were prepared with distilled deionized water (resistivity, ρ 18.2 MΩ × cm) purified by using a Millipore milli-Q-plus unit to remove organic and inorganic impurities, and subsequently passed through milli-Q-plus ion exchange columns. All experiments were performed in 0.1 mol × L^{-1} KCl solution saturated with Ar, O_2, or 5% H_2/95% Ar gas at pH 7 or 9.5. The temperature of the electrolyte was maintained at 60 °C.

2.4. Experimental procedure

Within the glass cell, E_{CORR} measurements were recorded for various lengths of time, but generally until a steady-state potential was achieved. These measurements were sometimes followed by cathodic stripping voltammetry (CSV). Each CSV sweep started at E_{CORR} and ended at −1.2 V (vs SCE). The potential scan rate was 2 mV/s.

Within the pressure vessel, after the cell was de-aerated with Ar, E_{CORR} was measured until a steady-state was reached. A fixed pressure of H_2 was then introduced into the vessel by pressurizing with a mixture of 5% H_2/95% Ar. Once E_{CORR} achieved a steady-state value, the H_2 content of the cell was changed and the cell allowed to achieve a new steady-state. These experiments employed mixed gas (5% H_2/95% Ar) total pressures of 0.034, 0.069, 0.14, 0.21, and 0.28 MPa.

3. Results and discussion

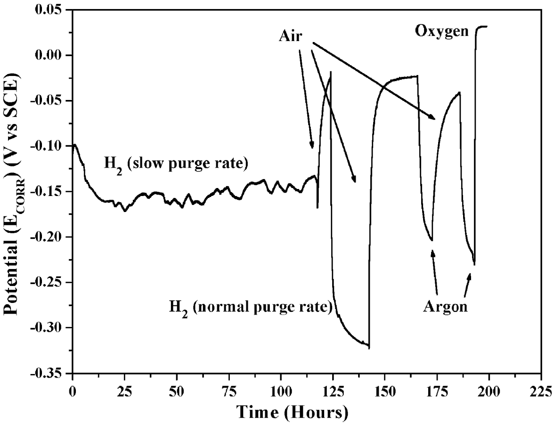

Fig. 4. E_{CORR} measurements on SIMFUEL electrodes with ε-particles as a function of time for solutions purged with various gases at 60 °C. The electrode was not potentiostatically cleaned prior to the start of the experiment.

Fig. 4 shows the E_{CORR} recorded on a SIMFUEL electrode with ε-particles in a glass cell purged with various gases at 60 °C. The electrode was not cleaned electrochemically, so a thin air-formed surface oxide was present on the UO_2 surface prior to the start off the experiment. It is clearly evident that the electrode responded differently to the solutions purged with different gases. Our measured E_{CORR} values can be related to the behaviour summarized in Fig. 3. In solutions saturated with air, E_{CORR} was at the threshold for U^{VI} production at ≈−40 mV; in O_2 saturated solutions, E_{CORR} (≈20 mV) was in the range expected for dissolution as UO_2^{2+} and the formation of a $UO_3 \cdot yH_2O$ deposit. In Ar-purged solutions, which represent anoxic conditions, E_{CORR} (≈−200 mV) was in the range of UO_{2+x} formation. The introduction of 5% H_2/95% Ar clearly exerted a reducing effect, polarizing the electrode to a potential (≈−300 mV) below that achievable under anoxic (Ar-purged) conditions. Also, when the 5% H_2/95% Ar-purge rate was varied, E_{CORR} also varied considerably. This variation in E_{CORR} with H_2-purge rate suggests the reaction of H_2 with the electrode surface is, at least partially, transport-controlled on the UO_2 surface. This suggests H_2 is consumed faster than it is replenished at the surface for a slow purge rate.

Fig. 5 shows the values of E_{CORR} measured on a SIMFUEL electrode with ε-particles in separate solutions purged with either Ar, O_2, or 5% H_2/95% Ar. In each case, the electrode was not cleaned potentiostatically prior to exposure to the solution, and would, therefore, be expected to have been covered by a thin air-formed surface oxide. In an O_2 environment, E_{CORR} was again ≈21 mV. This would imply that the oxidized fuel surface is stable in this environment. In the Ar-purged solution, E_{CORR} decreased with time, eventually obtaining a steady-state value of ≈−205 mV. This decrease with time can be attributed to the slow dissolution of the thin surface oxide present on the UO_2 surface to

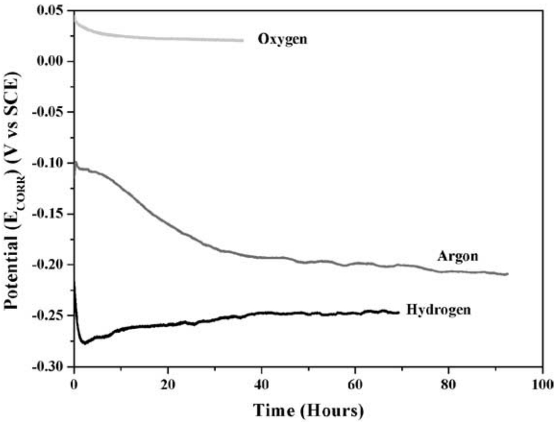

Fig. 5. E_{CORR} measurements on SIMFUEL electrodes with ε-particles in argon, oxygen, or hydrogen at 60 °C. The electrode was not cleaned potentiostatically before the start of each experiment.

produce a cleaner, less oxidized surface. When the solution was purged with 5% H_2/Ar, the electrode surface was immediately polarized to a value below that achieved under anoxic conditions in Ar. A steady state E_{CORR} of ≈−247 mV was obtained after 70 h. This demonstrates that the presence of H_2 suppresses the E_{CORR} of the electrode, and suggests H_2 has a reducing effect on SIMFUEL. However, it is not presently known whether any reduction of the oxidized surface layer occurs, although its redissolution, as observed in an Ar-purged system, would still be expected.

Fig. 6 shows a cyclic voltammogram on a SIMFUEL electrode with ε-particles recorded by scanning the potential of an electrochemically cleaned electrode from −1.2 V to +0.3 V and back at a scan rate of 5 mV/s. This current–potential relationship demonstrates the potential ranges within which the SIMFUEL surface can be oxidized (positive-going scan) and reduced (negative-going) scan. A detailed interpretation of such voltammograms on UO_2 and SIMFUEL has been given elsewhere [7,8], and only a brief description is included here. Although only shallow, the current increase on the positive-going scan for $E \geqslant -0.4$ V is attributable to the oxidation of the UO_2 surface ($UO_2 \rightarrow UO_{2+x}$), consistent with the redox summary in Fig. 3. The increase in current as the positive scan limit was approached was due to further oxidation to produce soluble UO_2^{2+} and, in 0.1 mol × L^{-1} KCl a $UO_3 \cdot yH_2O$ corrosion product deposit. On the reverse scan, reduction of the anodically formed oxide commenced for $E < -0.5$ V and the reduction of H_2O to H_2 accounts for the very large increase in cathodic current for $E \leqslant -0.9$ V [7,18,19]. According to Fig. 6, a potential <−0.5 V would be required to electrochemically reduce oxides formed by air oxidation or aqueous corrosion on a UO_2 (SIMFUEL) surface. As shown by the vertical arrow indicating the value of E_{CORR} (−247 mV) in 5% H_2/95% Ar-purged solution (from Fig. 5, on an air oxidized specimen), this did not occur.

An additional set of E_{CORR} measurements was performed on SIMFUEL electrodes with ε-particles after electrochemically cleaning the electrodes (at −1.6 V for 10 min) to remove any air-formed film that might be present, Fig. 7. The E_{CORR} values achieved were considerably lower in the case of O_2-purged (−38 mV compared to +21 mV) and 5% H_2/95% Ar-purged (−309 mV compared to −247 mV) solutions compared to the values recorded with an air-oxidized specimen,

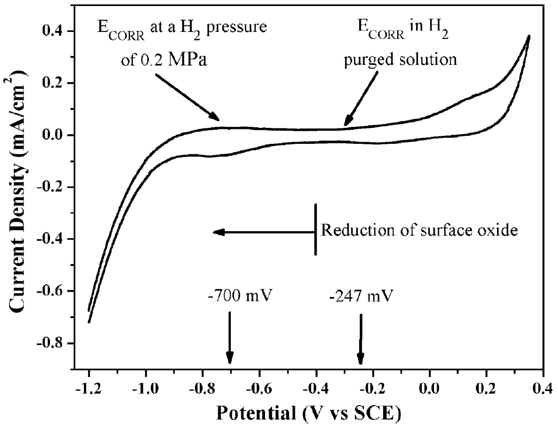

Fig. 6. Cyclic voltammogram on SIMFUEL electrodes with ε-particles recorded in 0.1 mol × L^{-1} KCl de-aerated with argon at 60 °C, scan rate 5 mV/s.

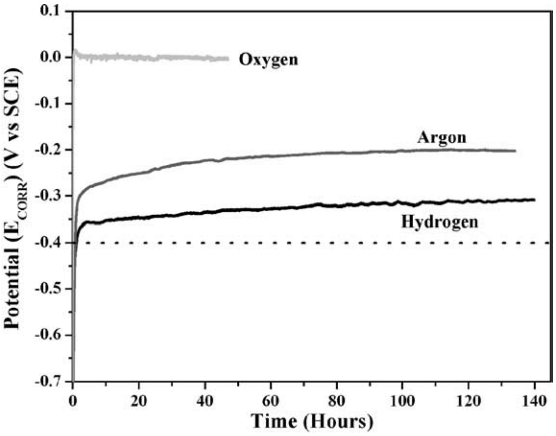

Fig. 7. Open circuit potential measurements on SIMFUEL electrodes with ε-particles in various gases at 60 °C. The electrode was potentiostatically cleaned prior to the start of each experiment. Dashed line refers to the threshold of surface oxidation/dissolution.

Fig. 5. For anoxic conditions (Ar-purged) the values were effectively the same (−203 mV compared to −209 mV). Also shown in Fig. 7 (dashed line) is the potential threshold for the oxidation of the UO_2 surface (to UO_{2+x}) (from Fig. 3). E_{CORR} for the 5% H_2/95% Ar-purged solution approached this boundary, suggesting that H_2 suppresses the oxidation of a clean UO_2 surface. That no significant oxidation of the UO_2 surface occurred in the experiment is supported by the observation that the steady-state E_{CORR} value was rapidly established once the cathodic polarization used to clean the electrode was removed.

Cathodic stripping voltammograms, Fig. 8, were performed on SIMFUEL electrodes with ε-particles to determine whether exposure to solutions purged with the various gases led to observable differences in the extent of surface oxidation. In these experiments the electrode was first cathodically cleaned to remove air-formed oxides and then allowed to achieve a steady-state E_{CORR} value in either an Ar or 5% H_2/95% Ar-purged solution. In Fig. 8, the arrows indicate the E_{CORR} values achieved prior to recording the CSV's. The CSV after exposure to an O_2-purge is not shown since a residual current for the reduction of traces of O_2 was also obtained making any attempts to measure an oxide reduction charge unreliable. Little difference in the CSV's was observed after purging with Ar or 5% H_2/95% Ar. This was not entirely unexpected, since the difference in E_{CORR} was small (≈50 mV). In both CSV's a current for the reduction of any surface oxide was barely discernable. Integrating the current from E_{CORR} to a potential of −780 mV gives a slightly lower charge after 5% H_2/95% Ar-purging than after Ar-purging. While observable, this difference is marginal and it is difficult to say whether the extent of surface oxidation was lower after exposure to the 5% H_2/95% Ar-purged solution than after exposure to Ar-purged solutions.

If the pressure of H_2 was increased, in experiments performed in the pressure vessel, E_{CORR} was found to be pressure-dependent over the range 0–0.21 MPa (total gas pressure, 5% H_2/95% Ar), eventually achieving a value of ≈−700 mV for a pressure of 0.21 MPa, Fig. 9. For higher pressures, further changes in E_{CORR} were marginal. As indicated by a second arrow in Fig. 5, such a potential would be low enough to cause the cathodic reduction of surface oxides. Comparison of this E_{CORR} value (≈−700 mV) to the redox conditions summarized in Fig. 3 shows that it is sufficiently negative to completely suppress UO_2 oxidation.

To determine whether or not the noble metal ε-particles present in SIMFUEL are involved in establishing the E_{CORR} value in the presence of H_2, we repeated E_{CORR} measurements on a SIMFUEL specimen that did not contain these particles, Fig. 10. The E_{CORR} value in the presence of H_2 was 143 mV less negative than that obtained on SIMFUEL with ε-particles, and effectively identical to that observed under anoxic conditions (Ar-purged) i.e., the ability of H_2 to polarize the SIMFUEL surface to a more negative redox condition was lost.

This difference in behaviours observed with and without ε-particles present indicates a clear role for these particles in suppressing the oxidation of UO_2. The most likely explanation is that the H_2 dissociation reaction is catalyzed on these particles, which act as galvanically-coupled anodes within the fuel matrix, leading to a decrease in E_{CORR} and inhibition of UO_2oxidation/corrosion. The reversible formation of adsorbed surface atoms on noble metal electrodes is well characterized in the electrochemical literature [20]. An attempt to

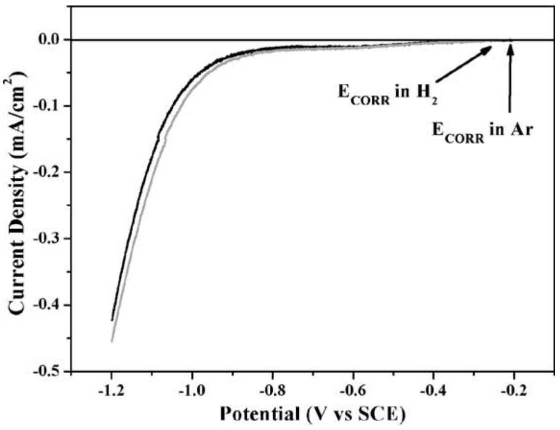

Fig. 8. Cathodic stripping voltammograms on SIMFUEL electrodes with ε-particles in solutions saturated with various gases after recording the E_{CORR} measurements at 60 °C, as shown in Fig. 4.

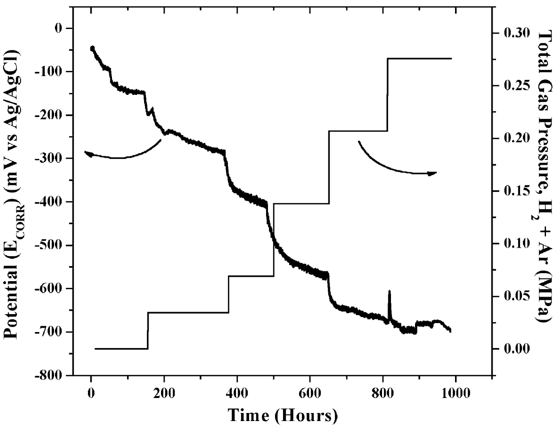

Fig. 9. E_{CORR} measured on SIMFUEL with ε-particles at 60 °C for various argon and hydrogen pressures. The system was initially purged with just argon at atmospheric pressure, then with a series of increasing 5% H_2/Ar pressures.

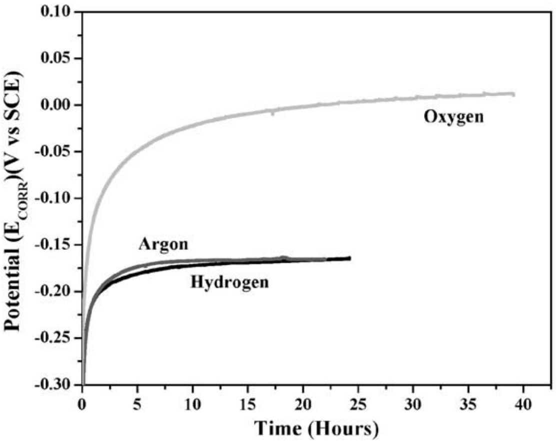

Fig. 10. Corrosion potentials in solutions saturated with various, gases using SIMFUEL without any ε-particles at 60 °C. The electrode was electrochemically cleaned before the start of each run.

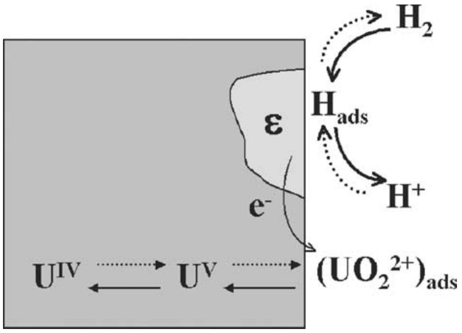

Fig. 11. Illustration of a galvanic coupling between the UO_2 matrix and ε-particles.

illustrate this process schematically is shown in Fig. 11. Although this schematic indicates that such a galvanic coupling can reduce oxidized U species (e.g., adsorbed U^{VI} species), definite proof that this can occur remains to be obtained. However, we expect that the conductivity of UO_2, and hence its ability to galvanically couple to the ε-particles over a substantial lateral range, is significantly enhanced by the presence of the trivalent rare-earth dopants in the fuel matrix.

Figs. 12 and 13 compare the short term response of SIMFUEL, with and without ε-particles, to H_2 and O_2, respectively. In the presence of H_2, the time taken to approach steady-state on the two electrodes was not very different. The response when ε-particles were present shows a slight arrest around −750 mV, which coincides with the potential for the onset of H_2O reduction, Fig. 8. While this could be taken as an indication of H_2 oxidation on ε-particles, its reproducibility needs to be confirmed.

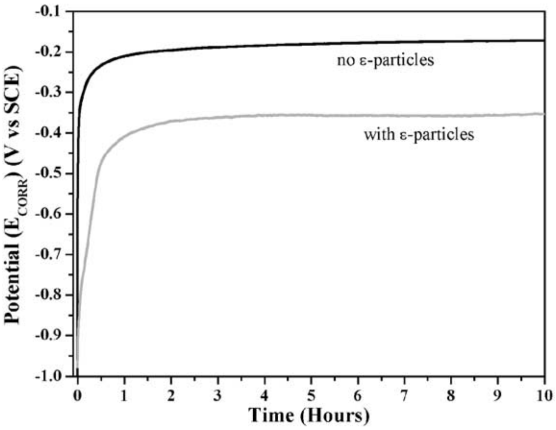

Fig. 12. E_{CORR} in solutions saturated with 5% H_2/95% Ar on SIMFUEL with and without ε-particles.

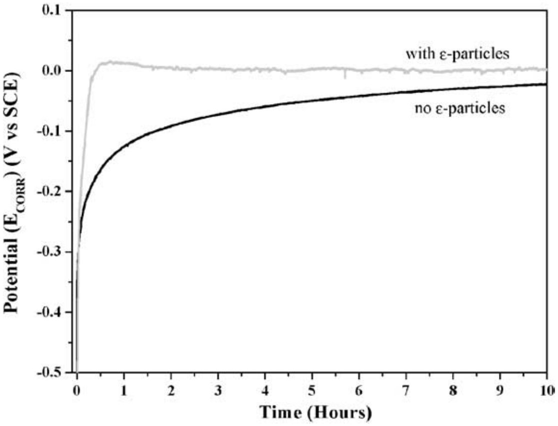

Fig. 13. E_{CORR} in solutions saturated with oxygen on SIMFUEL with and without ε-particles.

By contrast, there was a very clear difference in the response of the electrode with and without ε-particles in an O_2-purged solution. The relatively slow establishment of steady-state on UO_2 has been attributed to the slow kinetics of the O_2 reduction reaction on unoxidized surfaces on the fuel corrosion process [18,21]. The very rapid response when ε-particles were present could be due to a catalysis of the O_2 reduction reaction on these particles and an overall acceleration of the fuel oxidation/corrosion process. An unsubstantiated claim that ε-particles are involved in O_2 reduction on SIMFUEL has previously been made [22].

4. Conclusions

Dissolved H_2 suppresses the E_{CORR} of a simulated spent fuel surface (SIMFUEL) to a value below that achieved in anoxic (Ar-purged) solutions. Experiments on electrodes with and without noble metal ε-particles indicate that the formation of reductive radicals by H_2 oxidation may be catalyzed on these ε-particles, which act like galvanically-coupled cathodes within the fuel matrix. This leads to a decrease in corrosion potential (E_{CORR}) and inhibition of UO_2 oxidation. On SIMFUEL with ε-particles, at higher total gas pressures (5% H_2/95% Ar, 0.21 MPa), the E_{CORR} is suppressed to values sufficiently negative that the reduction of oxidized U species could occur. O_2 reduction may also be catalyzed on the ε-particles, which causes an increase in E_{CORR}. Whether the reaction $U^{V}/U^{VI} + H^{\cdot} \rightarrow U^{IV}$ occurs remains to be proven.

Acknowledgements

This research is funded under the Industrial Chair agreement between the Canadian Natural Sciences and Engineering Research Council (NSERC) and Ontario Power Generation (OPG), Toronto, Canada.

References

[1] J. McMurry, D.A. Dixon, J.D. Garroni, B.M. Ikeda, S. Stroes-Gascoyne, P. Baumgartner, T.W. Melnyk, Ontario Power Generation Report No: 06819-REP-01200-10092-R00, 2003.

[2] F. King, M. Kolar, Mater. Res. Soc. Symp. Proc. 412 (1996) 547.

[3] S.Sunder, Atomic Energy of Canada Limited Report, AECL-11380, COG-95-340, 1995.

[4] F. King, M. Kolar, Ontario Power Generation Report No: 00819-REP-01200-10041-ROO, 1999.

[5] L.H. Johnson, D.M. LeNeveu, F. King, D.W. Shoesmith, M. Kolar, D.W. Oscarson, S. Sunder, C. Onofrei, J.L. Crosthwaite, Atomic Energy of Canada Limited Report, AECL-11494-2, COG-95-552-2, 2000.

[6] D.W. Shoesmith, M. Kolar, F. King, Corrosion 59 (2003) 802.

[7] D.W. Shoesmith, J. Nucl. Mater. 282 (2000) 1.

[8] B.G. Santos, H.W. Nesbitt, J.J. Noël, D.W. Shoesmith, Electrochim. Acta 49 (2004) 1863.

[9] J.D. Rudnicki, R. Russo, D.W. Shoesmith, J. Electroanal. Chem. 372 (1994) 3.

[10] K. Spahiu, L. Werme, U.-B. Eklund, Radiochim. Acta 88 (2000) 507.

[11] S. Röllin, K. Spahiu, U.-B. Eklund, J. Nucl. Mater. 297 (2001) 231.

[12] J.C. Tait, L.H. Johnson, in: Proceedings of the 2nd Canadian Nuclear Society, Toronto, 1986, p. 611.

[13] S. Sunder, G.D. Boyer, N.H. Miller, J. Nucl. Mater. 175 (1990) 147.

[14] F. King, M.J. Quinn, N.H. Miller, Swedish Nuclear Fuel Company (SKB) Report, SKB TR-99-27, 1999.

[15] P.G. Lucuta, R.A. Verrall, H. Matzke, B.J. Palmer, J. Nucl. Mater. 178 (1991) 48.

[16] A.F. Gerwing, F.E. Doern, W.H. Hocking, Surf. Interface Anal. 14 (1989) 559.

[17] X. He, J.J. Noël, D.W. Shoesmith, J. Electrochem. Soc. 149 (9) (2002) B440.

[18] D.W. Shoesmith, W.H. Hocking, J.S. Betteridge, Ontario Power Generation Report No: 06819-REP-01200-10052-ROO, 2001.

[19] D.W. Shoesmith, S. Sunder, W.H. Hocking, in: J. Lipkowski, P.N. Ross (Eds.), Electrochemistry of Novel Materials, vol. 29, VCH, New York, 1996, Chapter 6.

[20] S. Trasatti, J. Electroanal. Chem. 39 (1977) 163; Electrochim. Acta 39 (1994) 1739.

[21] D.W. Shoesmith, S. Sunder, M.G. Bailey, G.J. Wallace, Corros. Sci. 29 (1989) 1115.

[22] J.S. Betteridge, N.A.M. Scott, D.W. Shoesmith, L.E. Bahen, W.H. Hocking, P.G. Lucuta, Atomic Energy of Canada Report, AECL-11647, COG-96-331-I, 1999.